Supplementary Table 1.

Mass Cytometry Panel				
Channel	Target	Clone	Vendor	Extracellular (E) or Intracellular (I)
Y89Di	CD45	HI30	Fluidigm	E
Nd142Di	CD19	HIB19	Fluidigm	E
Nd143Di	CD45RA	HI100	Fluidigm	E
Nd144Di	CD31	WM58	Fluidigm	E
Nd145Di	CD4	RPA-T4	Fluidigm	E
Nd148Di	CD274	29E.2A3	Fluidigm	E
Sm149Di	CD45RO	UCHL1	Fluidigm	E
Nd150Di	CD86	IT2.2	Fluidigm	E
Sm154Di	CD3	UCHT1	Fluidigm	E
Gd158Di	CD33	WM53	Fluidigm	E
Gd160Di	TBET	4B10	Fluidigm	I
Dy161Di	CD90	5E10	Fluidigm	E
Dy162Di	CD8A	RPA-T8	Fluidigm	E
Ho165Di	CD223	11C3C65	Fluidigm	E
Er167Di	GATA3	TWAJ	Fluidigm	I
Er168Di	CD127	A019D5	Fluidigm	E
Tm169Di	CD25	2A3	Fluidigm	E
Er170Di	HLA-DR	L243	Fluidigm	E
Yb171Di	KI67	Ki-67	Biolegend*	I
Yb174Di	CD279	EH12.2H7	Fluidigm	E
Lu175Di	CD14	M5E2	Fluidigm	E
Yb176Di	CD56	NCAM16.2	Fluidigm	E
Ir191Di	DNA Intercalator	N/A	Fluidigm	I
Ir193Di	DNA Intercalator	N/A	Fluidigm	I
Pt195Di	Cisplatin (viability)	N/A	Fluidigm	N/A
Bi209Di	CD11b	ICRF44	Fluidigm	E

*custom conjugated, included in panel but did not validate

Supplementary Figure 1

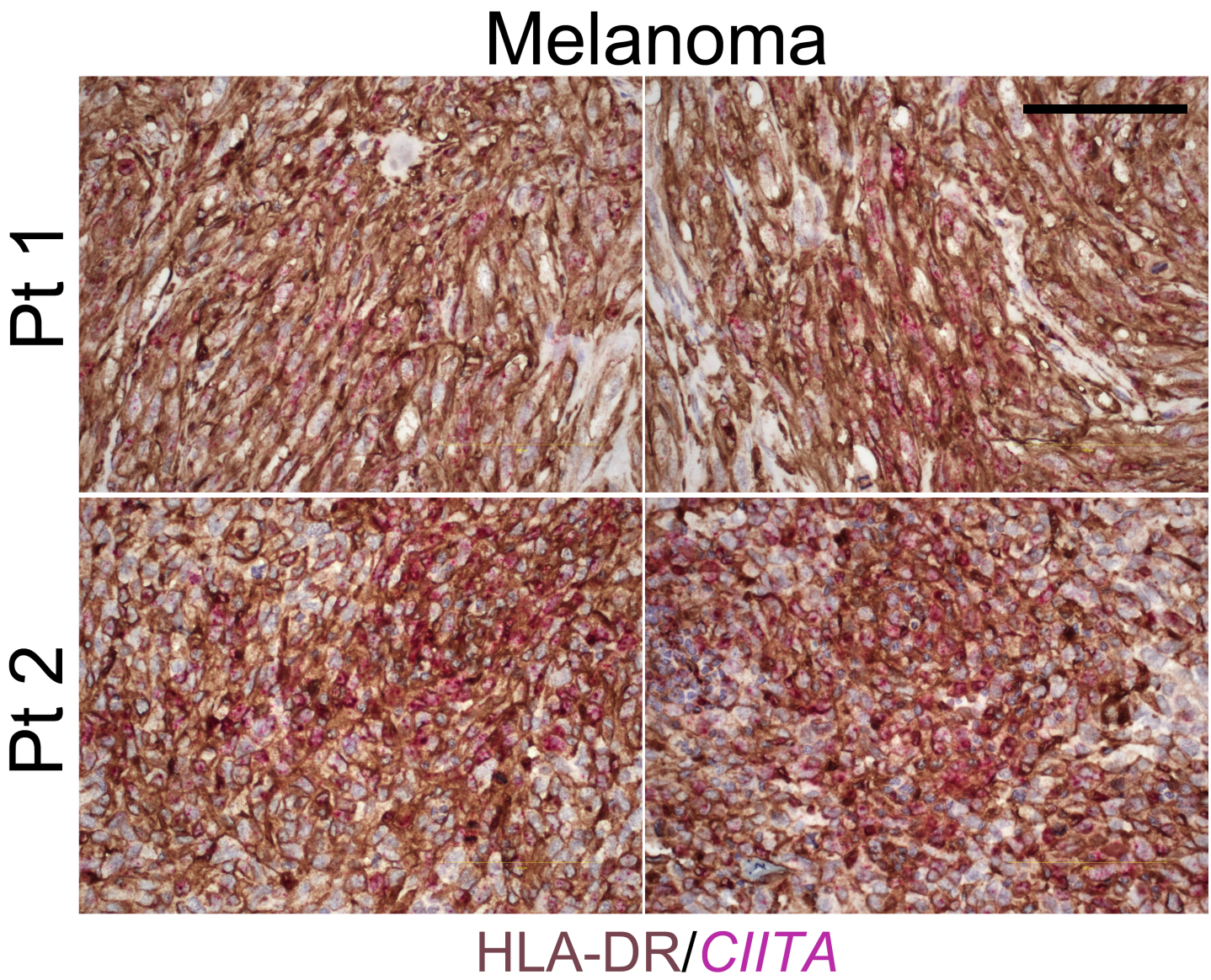

Supplementary Figure 1: MHC-II/HLA-DR expression by melanoma cells colocalizes with CIITA mRNA expression. Dual RNAish (*CIITA*, pink) and IHC (HLA-DR, brown) colocalizes on the same cells, suggesting that MHC-II expression is endogenous and represents a tumor cell autonomous phenotype rather than a result of trogocytosis.

Supplementary Figure 2

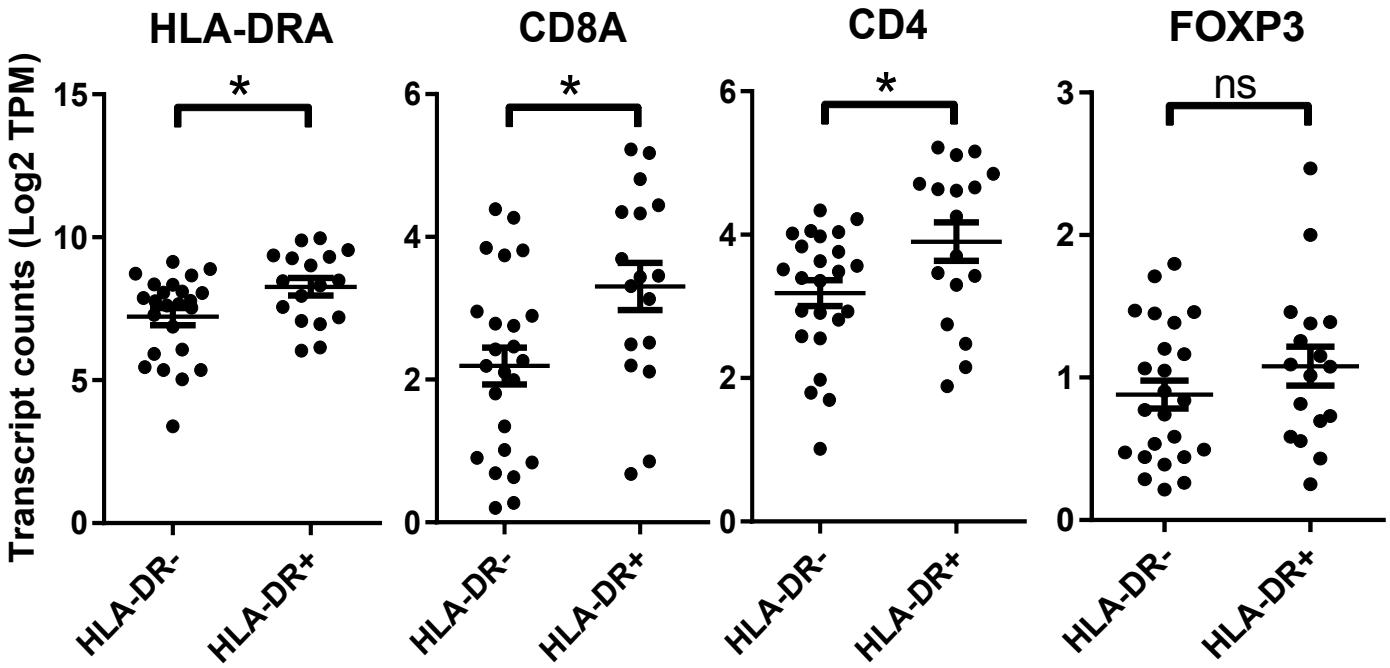

Supplementary Figure 2: MHC-II gene expression and T cell markers signatures by tumor-specific HLA-DR status (IHC). RNAseq expression levels of *HLA-DRA*, CD8A, CD4, and Foxp3 genes in MHC-II/HLA-DR+ tumors (>5% tumor cells positive) versus negative. *p<0.05 two-tailed t test.

Supplementary Figure 3

A

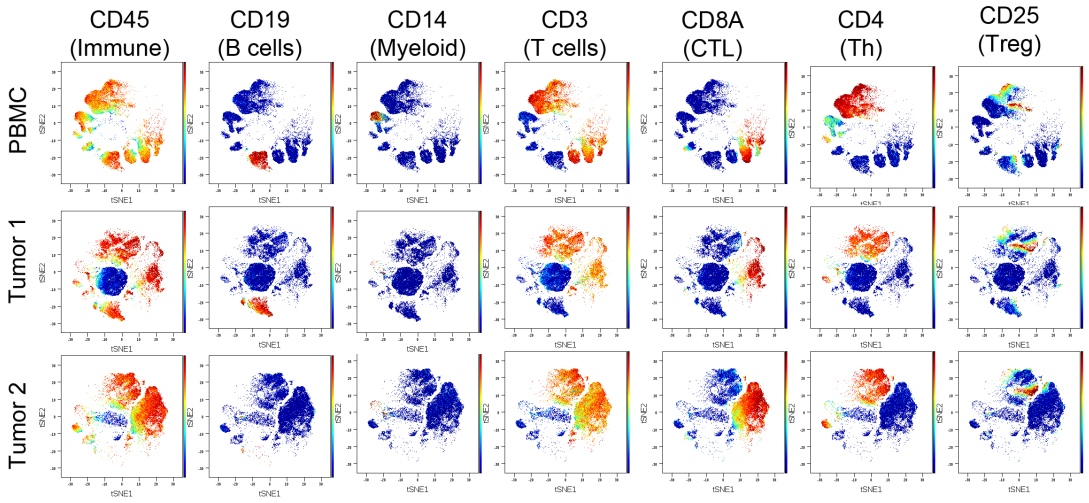

B

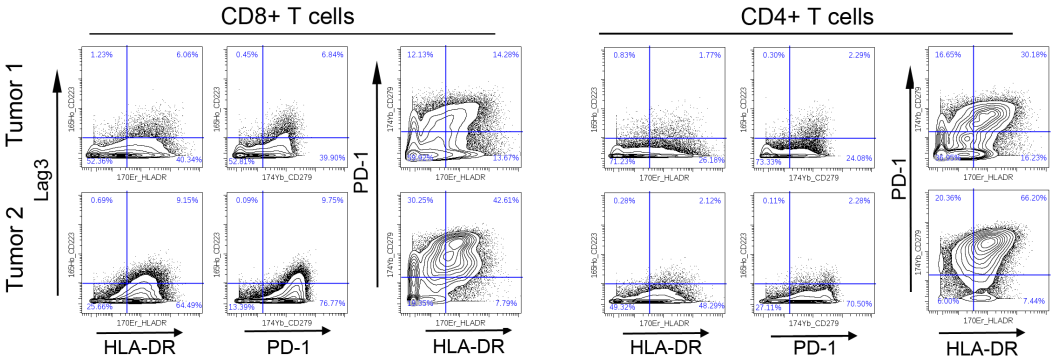

Supplementary Figure 3: CyTOF analysis of human melanomas. (A) Two freshly resected human melanomas were dissociated and analyzed by CyTOF using an immune contexture-based mass cytometry panel. Healthy human PBMCs were utilized as a control. ViSNE analysis was used to identify T cell populations and the expression of phenotypic markers within those populations. Scaled expression is represented by each color bar specific to the depicted marker. (B) Biplots demonstrating overlapping populations of HLA-DR, LAG3, and PD-1 on T cells in the melanoma specimens from (A).

Supplementary Figure 4

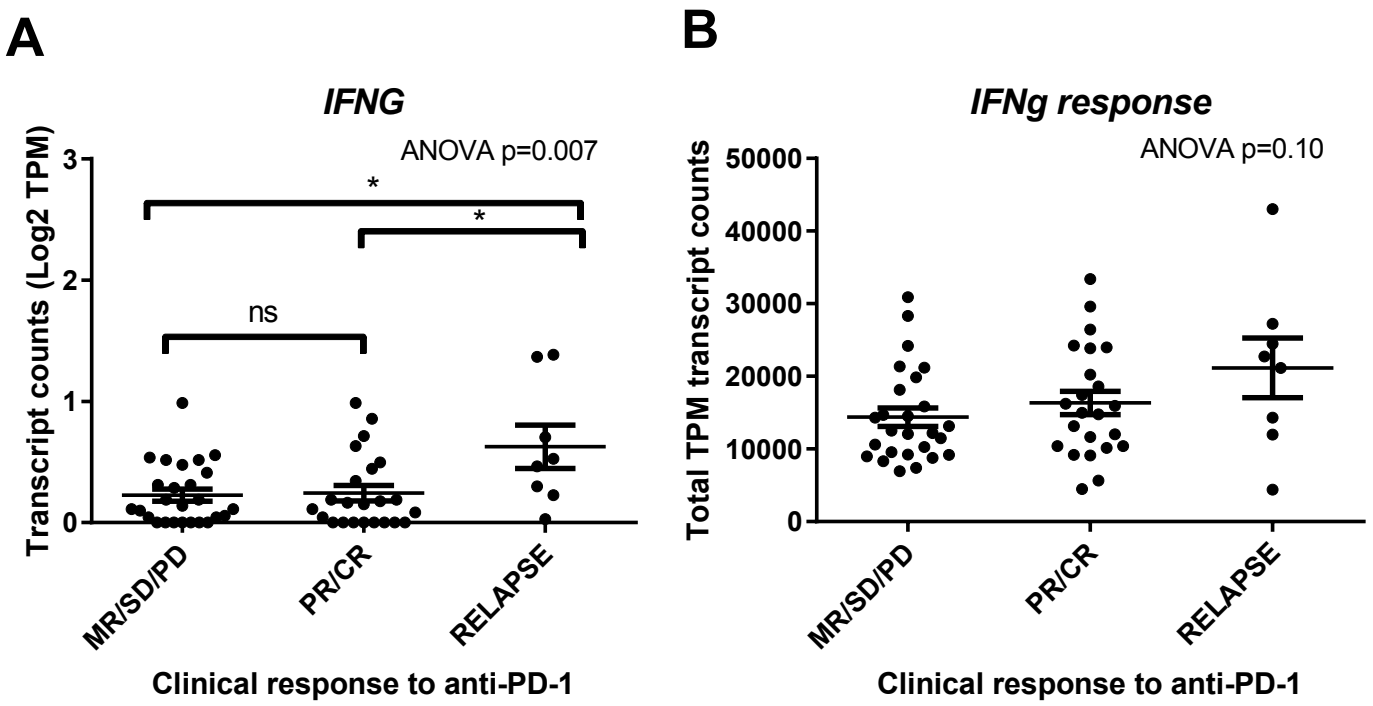

Supplementary Figure 4: Interferon-gamma gene expression signatures by outcome in PD-1 treated patients. RNAseq expression levels of *IFN-γ* (A) and IFN-γ-responsive (B) gene signatures by melanoma and lung patient irRC. *p<0.05, Tukey's post-hoc test.

Supplementary Figure 5

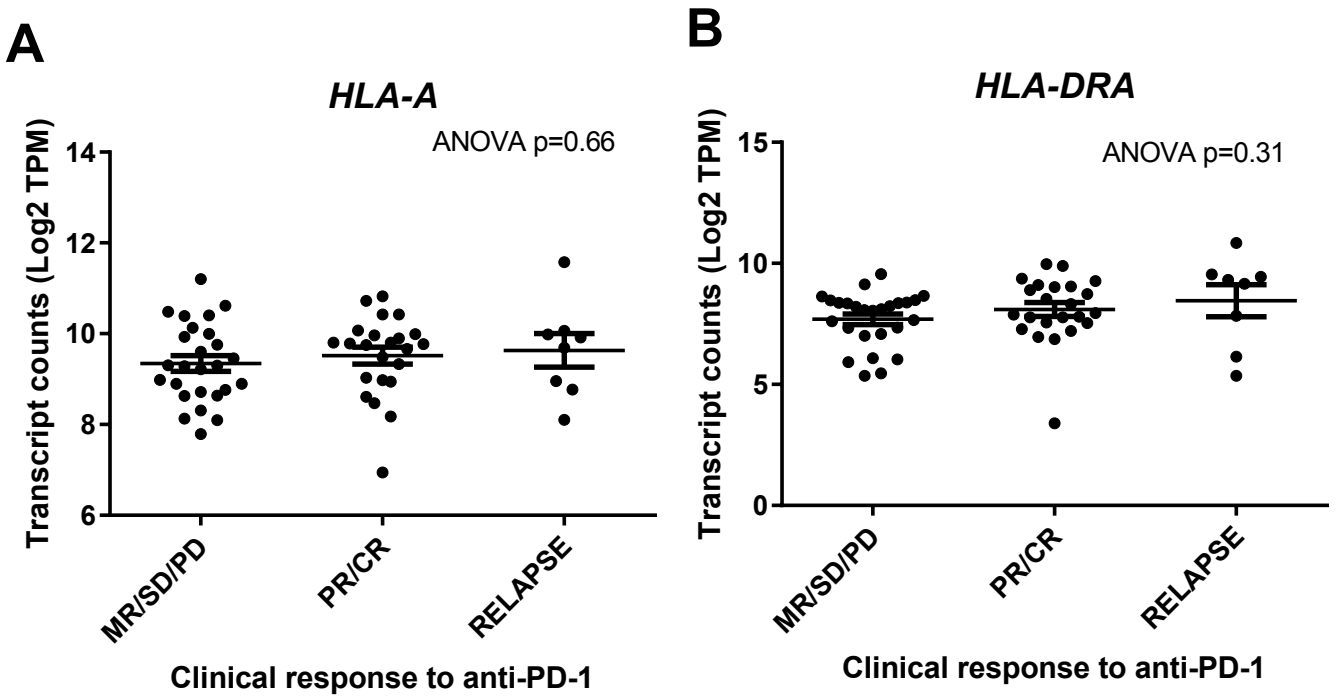

Supplementary Figure 5: MHC-I and MHC-II gene expression signatures by outcome in PD-1 treated patients. RNAseq expression levels of *HLA-A* (A) and *HLA-DRA* (B) genes by melanoma and lung patient irRC.

Supplementary Figure 6

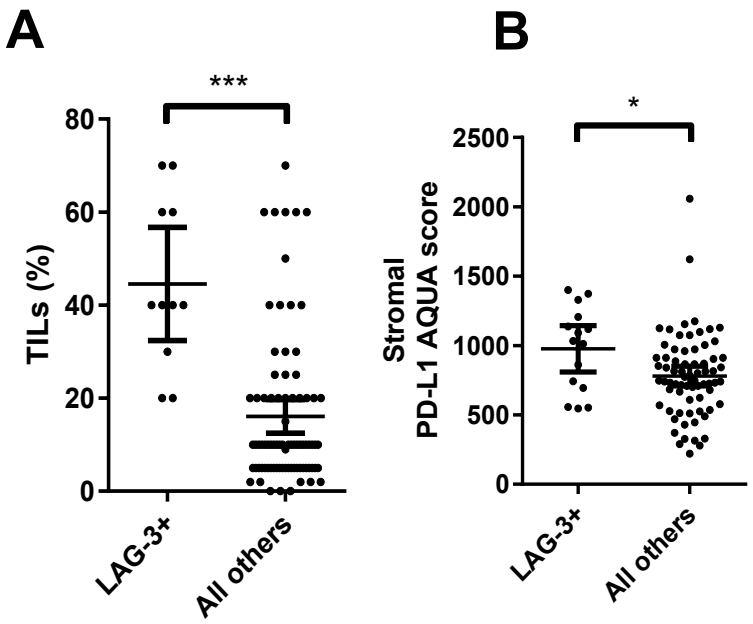

Supplementary Figure 6: Correlates of LAG-3+ TILs in TNBC. A) Percent-tumor infiltrating lymphocytes across TNBC patients, stratified by the presence of LAG-3+ cells. *** $p<0.001$; Mann Whitney U test. B) Percent- PD-L1+ stroma (AQUA score) across TNBC patients, stratified by the presence of LAG-3+ cells. * $p<0.05$; Mann Whitney U test.

Supplementary Figure 7

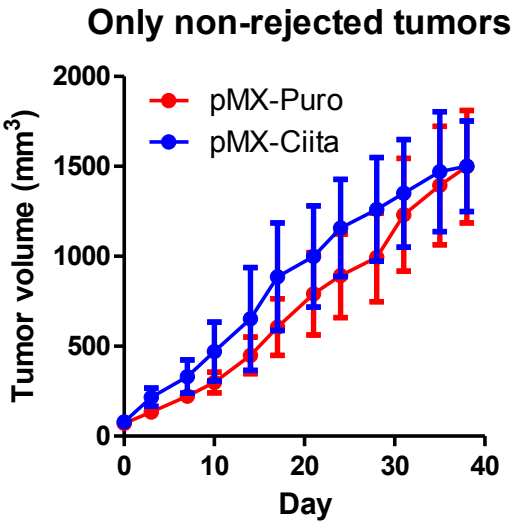

Supplementary Figure 7: No change in Ciita+ MMTV-neu tumor growth rate after immunologic escape. Tumor growth rates in MMTV-neu Ciita+ and puro-control tumors. Only mice which formed tumors (did not reject) are included.

Supplementary Figure 8

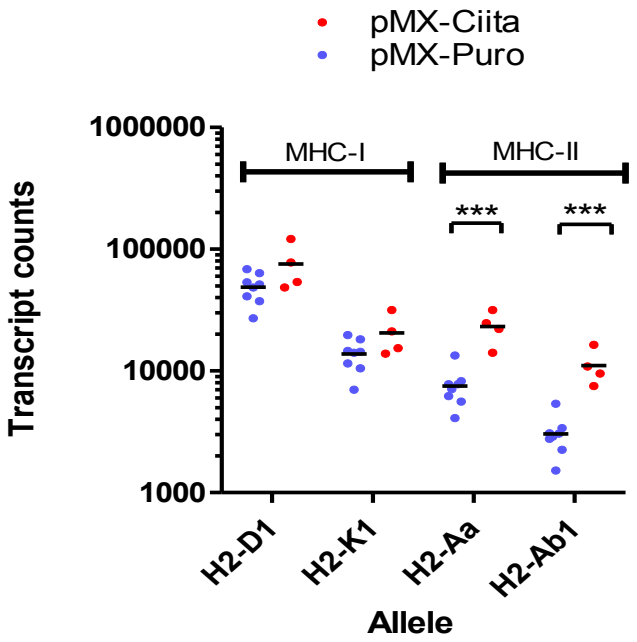

Supplementary Figure 8: Tumors escaping immunologic rejection in enforced- MHC-II expressing MMTV-neu tumors retain MHC-II expression. NanoString analysis of MHC-I and MHC-II gene expression in pMX-puro and pMX-Ciita transduced tumor cells from tumors harvested following tumor establishment.

Supplementary Figure 9

A

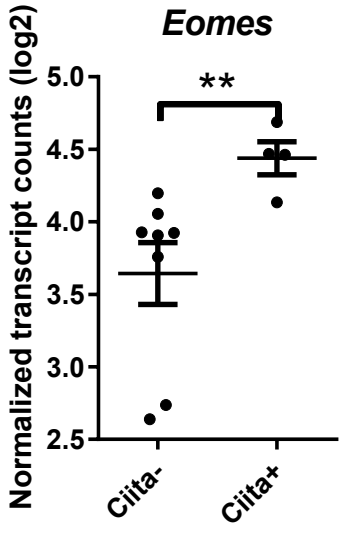

MMTV-neu tumors (*in vivo*)

B

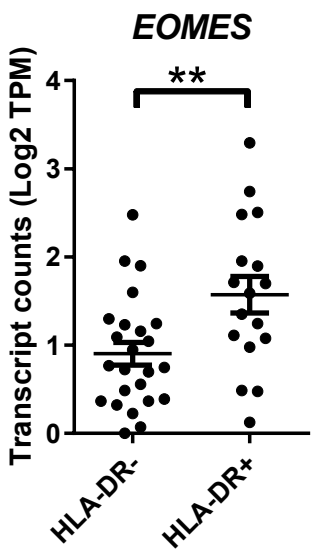

Human metastatic melanoma and lung cancer

Supplementary Figure 9: Higher eomesodermin expression in MHC-II+ tumors. A) NanoString analysis of eomesodermin gene expression in pMX-puro and pMX-Ciita transduced tumor cells from tumors harvested following tumor establishment. B) Eomesodermin gene expression as measured by RNAseq in melanoma and lung cancer patients, stratified by MHC-II status. **p<0.01; Mann Whitney U test.

Supplementary Figure 10

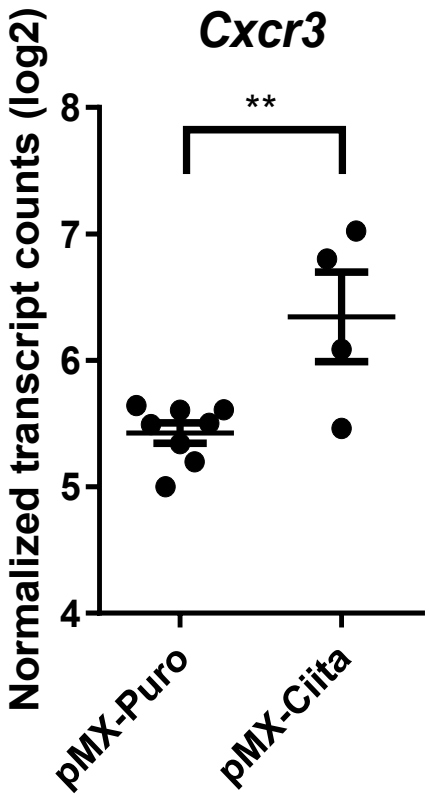

Supplementary Figure 10: Tumors escaping immunologic rejection in enforced MHC-II-expressing MMTV-neu tumors demonstrate higher CXCR3+ infiltrates. NanoString analysis of *Cxcr3* gene expression in pMX-puro and pMX-Ciita transduced tumor cells from tumors harvested following tumor establishment. ** $p<0.01$ two-sample t test.

Supplementary Figure 11

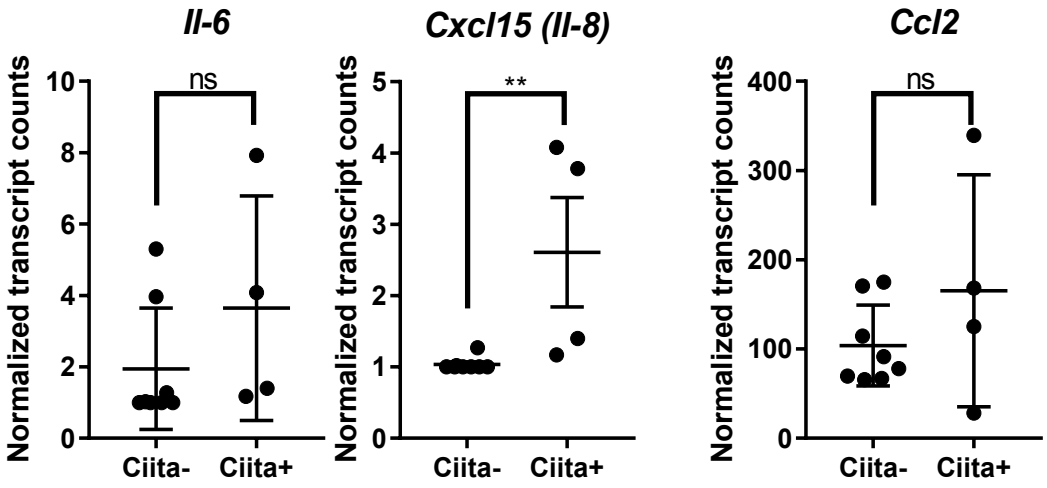

Supplementary Figure 11: Variable expression of myeloid cell chemoattractants in Ciita+ tumors. NanoString analysis of *Cxcr3* gene expression in pMX-puro and pMX-Ciita transduced tumor cells from tumors harvested following tumor establishment. ** $p<0.01$ two-sample t test.

Supplementary Figure 12

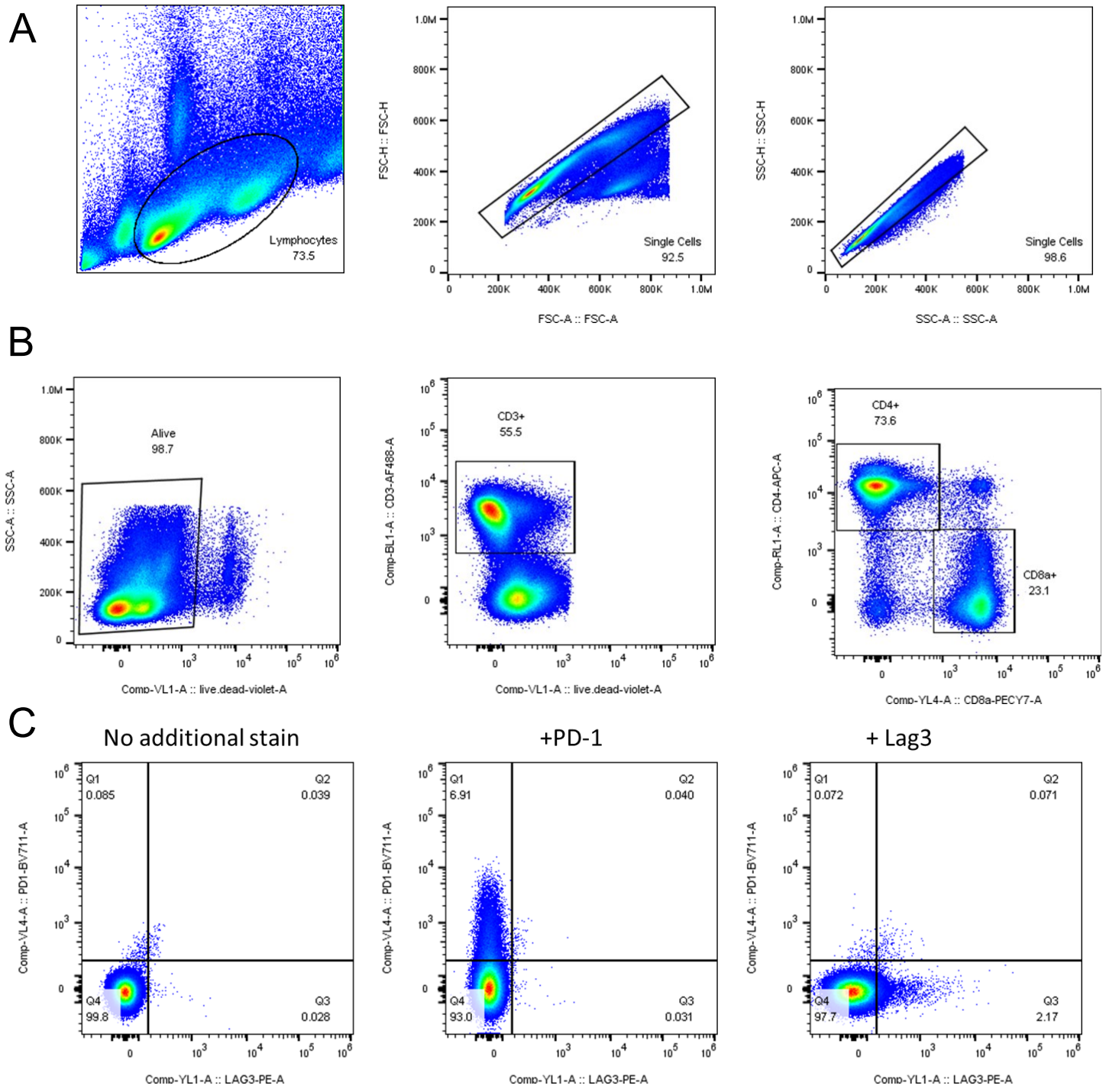

Supplementary Figure 12: Gating strategy. A) Pulse geometry for identifying/enriching single-cell lymphocytes. B) Identification of CD4/CD8+ T cells. C) Fluorescence-minus-one controls for PD-1+ CD3 cells and Lag3+ CD3 cells (Gated on CD3+ cells for FMO controls). Left—CD3+ cells with no PD-1 or Lag3 antibody. Middle— CD3+ cells with only PD-1 antibody. Right—CD3+ cells with only Lag3 antibody.

Supplementary Figure 13

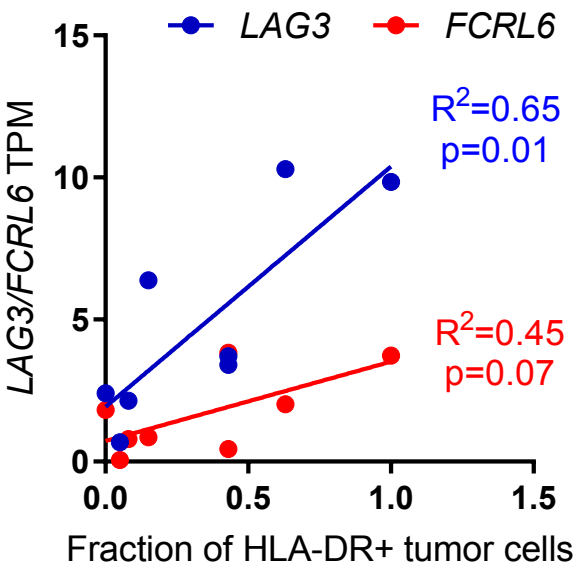

Supplementary Figure 13: Association of MHC-II receptor gene expression with degree of MHC-II positivity on tumor cells. RNAseq TPM counts for *CD233/LAG-3* and *FCRL6* were regressed and correlated to the fraction of HLA-DR+ tumor cells in the same specimen.

Supplementary Figure 14

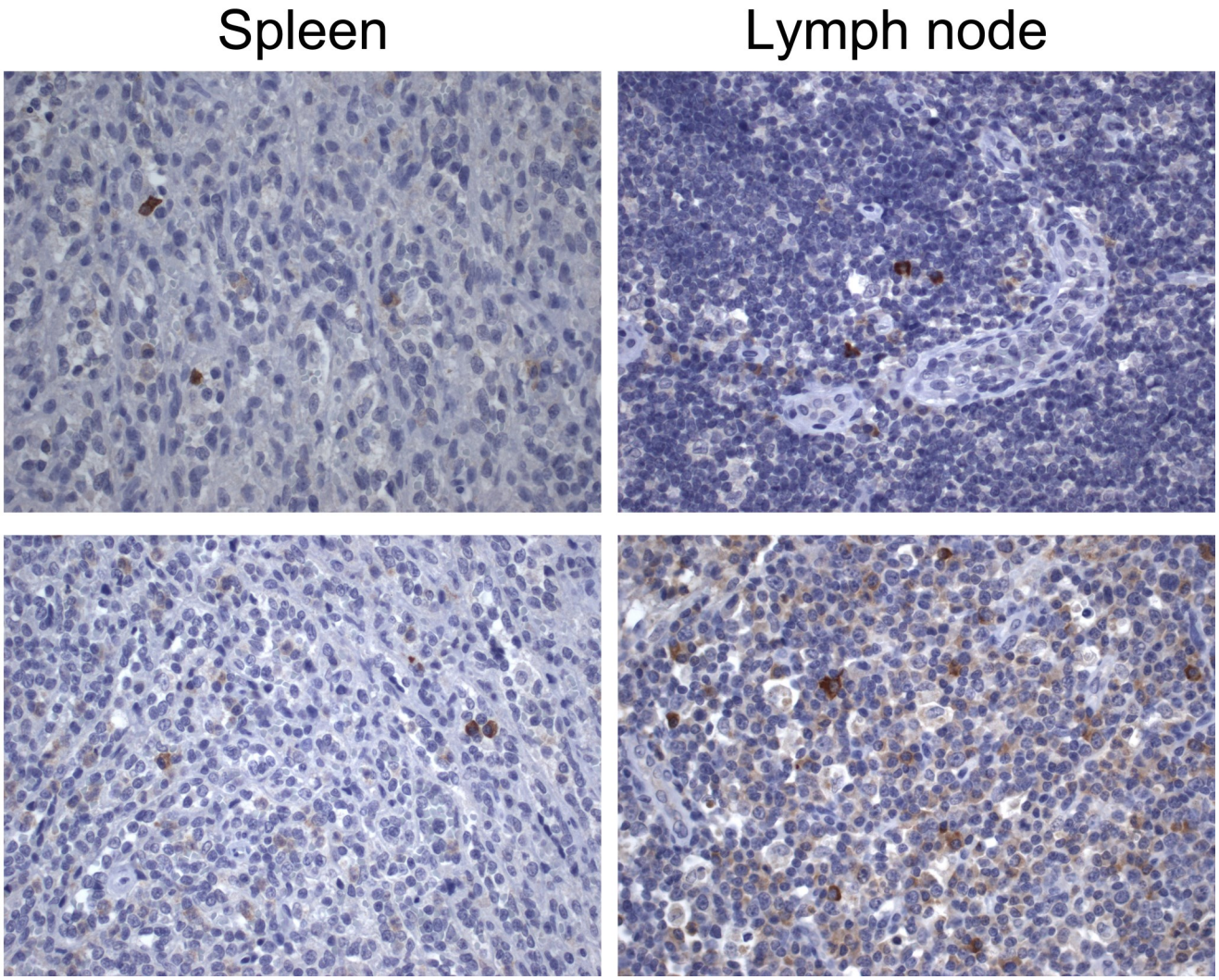

Supplementary Figure 14: Representative FCRL6 IHC staining. Human spleen and lymph node tissue sections were used to validate IHC staining for FCRL6, according to the reported methods.

Supplementary Figure 15

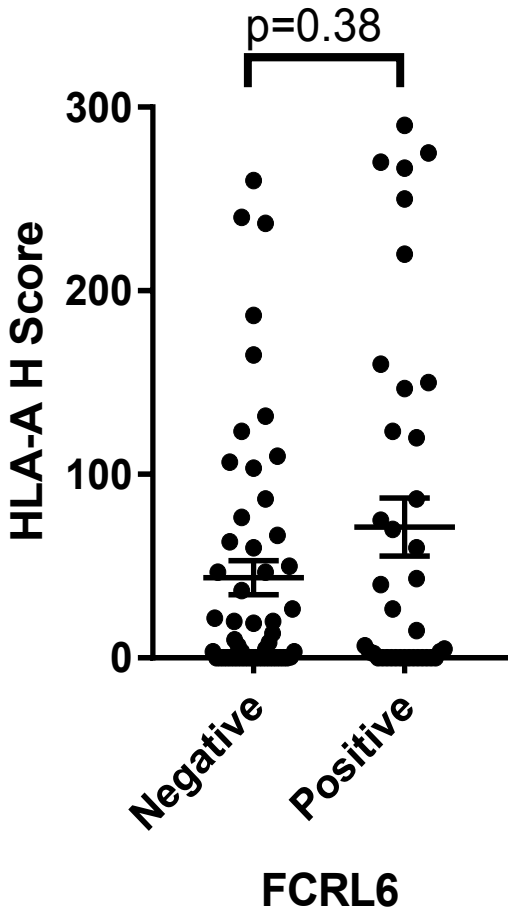

Supplementary Figure 15: No association of FCRL6+ TILs and MHC-I (HLA-A) expression on tumor cells. No association was detected between the presence of FCRL6+ TILs and HLA-A expression on tumor cells (H-score; intensity [0-3+] * fraction of tumor cells staining positive).

Supplementary Figure 16

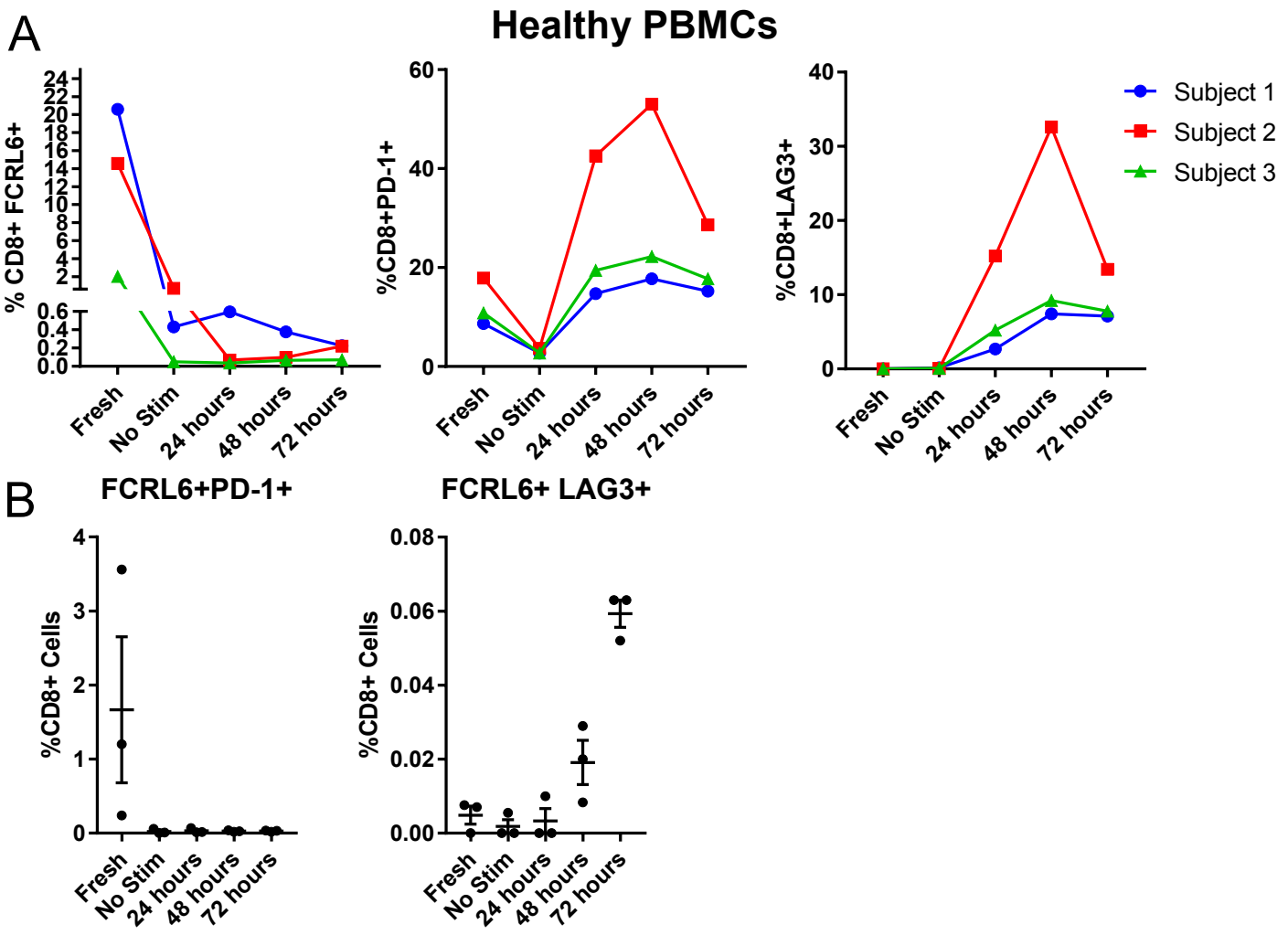

Supplementary Figure 16: Expansion of FCRL6+/LAG3+ CD8 T cells following TCR stimulation. A) Healthy human subject PBMCs were cultured with anti-CD3/CD28 beads for 24, 38, or 72 hours (or 72 hours without stimulation) and assayed by flow cytometry for CD8, FCRL6, PD-1, and LAG3. B) Co-expression of FCRL6 and PD-1 or FCRL6 and LAG3 on CD8 T cells in experiments from (A).

Supplementary Figure 17

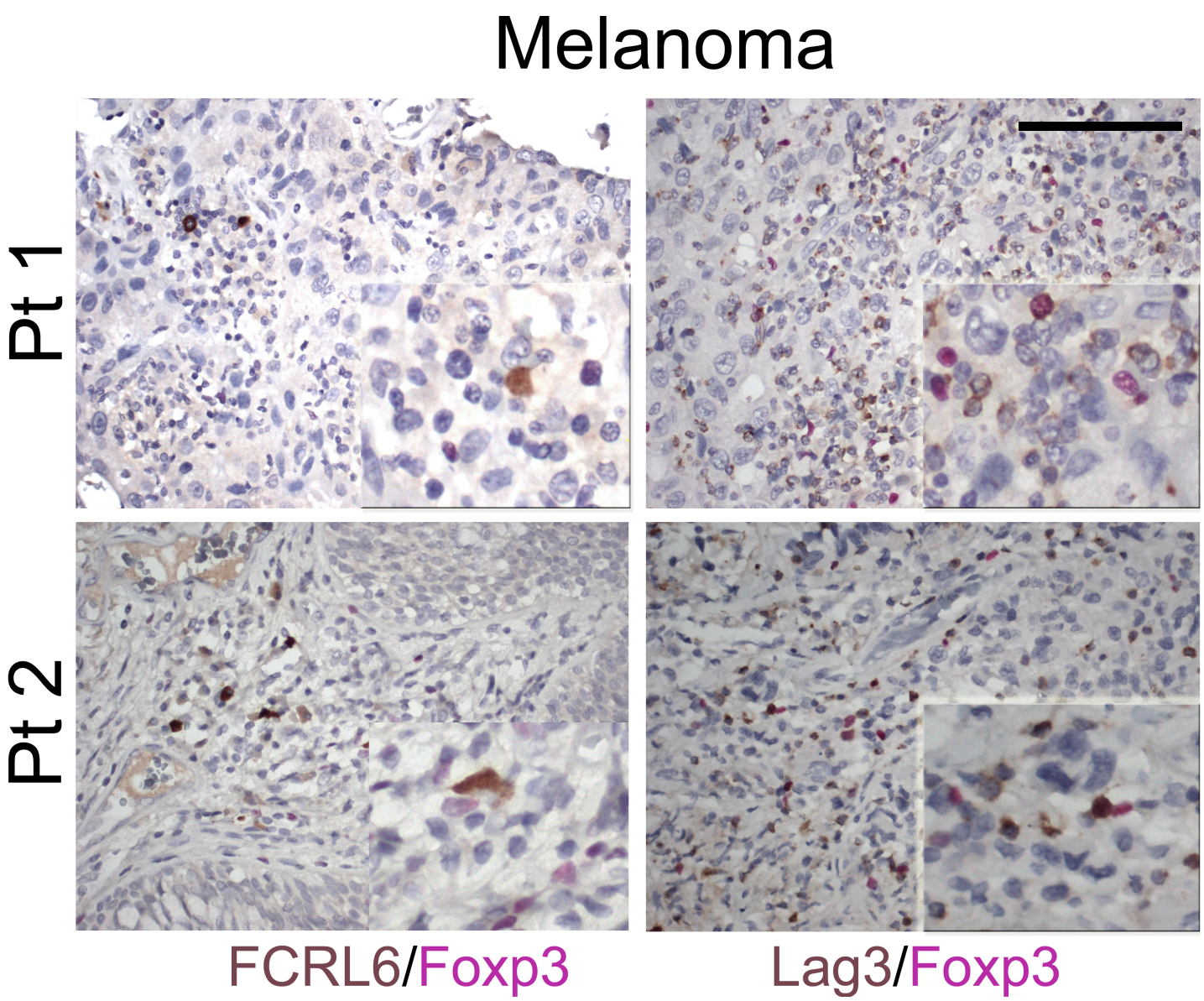

Supplementary Figure 17: FCRL6 and LAG3 do not colocalize with Foxp3+ regulatory T cells. No colocalization is observed by dual IHC for FCRL6 and Foxp3 or Lag3 and Foxp3 in human melanomas. While representative images are presented, a complete pathology analysis of the tissue produced no conclusively dual-positive cells.